AJNR

Optimization of gradient-echo MR for calcium detection.

M Henkelman and W Kucharczyk

AJNR Am J Neuroradiol 1994, 15 (3) 465-472
http://www.ajnr.org/content/15/3/465

Optimization of Gradient-Echo MR for Calcium Detection

Mark Henkelman and Walter Kucharczyk

PURPOSE: To determine optimal MR gradient-echo sequences for the visualization of calcium in neurologic MR. **METHOD:** The dependence of signal intensity and image contrast on the imaging parameters repetition time, echo time, flip angle, and spoiling were measured for hydroxyapatite samples. Calculations of signal intensity were shown to correspond to these measures. **RESULTS:** Optimum detectibility was obtained with an echo time of 29 msec and was independent of spoiling. As repetition time ranged from 30 msec to 700 msec, the optimal flip angle ranged from 17° to 66°. **CONCLUSIONS:** Gradient-echo sequences that optimize the contrast for detection of calcium in neurologic imaging have been determined.

Index terms: Brain, calcification; Brain, magnetic resonance; Magnetic resonance, gradient-echo; Magnetic resonance, technique; Magnetic resonance, tissue characterization

AJNR Am J Neuroradiol 15:465–472, Mar 1994

The effect of calcium on tissue signal intensity in magnetic resonance (MR) is variable (1–6). Calcified tissue may be hypointense, isointense, or hyperintense depending on the concentration of the calcium, surface area of the calcium particles, and the MR technique used. Isointense calcified lesions, that is, those that have signal intensity similar to that of surrounding tissue, pose a particularly difficult diagnostic problem. They may be overlooked entirely or the presence of calcium within the lesion may not be appreciated. In the former case, the result is a false-negative examination, in the latter case, a finding of potential differential diagnostic significance is lost. Clearly, the ability to determine the presence or absence of calcium in tissue is diagnostically beneficial.

Gradient-echo imaging has been shown to be more effective than spin-echo techniques in the detection of calcium (1). Calcified structures are more consistently demonstrated, typically as hypointense regions in the image. The hypointensity is caused by the low proton density of calcified tissue and, more importantly, by the dephasing imparted to water protons in the local magnetic gradients created by the differences in magnetic susceptibility around calcium particles. Because gradient-echo techniques lack refocusing radiofrequency pulses, intravoxel dephasing accumulates, making the lesions appear dark. Diffusion of spins through these inhomogeneities, which is the dominant mode of signal loss on spin-echo imaging, is completely masked by intravoxel dephasing in gradient-echo imaging. The greater the degree of hypointensity of the calcified tissue compared with surrounding normal tissue, the more obvious it will be. It is the purpose of this paper to examine the dependence of signal intensity and image contrast on repetition time (TR), echo time (TE), flip angle, and spoiling at different calcium concentrations and to compare the experimental results with theoretical predictions. Recommendations are then made on an optimal MR technique for the detection of calcium with gradient-echo imaging.

Materials and Methods

A phantom was constructed consisting of 8 tubes (27 mm diameter) containing calcium hydroxyapatite (BDH Chemicals, Poole, England),

Received March 12, 1993; accepted pending revision May 3; revision received May 24.

From the Department of Medical Biophysics (M. H.) and Radiology (W. K.), University of Toronto, Ontario, Canada.

Address reprint requests to Walter Kucharczyk, MD, FRCP(C), Department of Radiology, University of Toronto, Room 127 FitzGerald Building, 150 College Street, Toronto, Ontario, M5S 1A8 Canada.

AJNR 15:465–472, Mar 1994 0195-6108/94/1503–0465

uniformly suspended in 2% agarose gel to avoid sedimentation. Concentrations varied from 0 to 350 mg of calcium per milliliter of suspending medium in steps of 50 mg/mL covering the clinically relevant range of concentrations determined from computed tomography. The tubes were immersed in a water bath to minimize macroscopic susceptibility effects. The calcium hydroxyapatite, herein referred to simly as *calcium*, is a powder with average grain size of 10 μm and solid density of 2.18 g/mL and surface area of 67 m^2/g.

All imaging was performed on a whole-body MR imager operating at 1.5 T (Signa General Electric Medical Systems, Milwaukee, Wis). Single sections in the coronal plane were imaged with the following parameters: field of view 20 cm, 256 × 256 resolution, various acquisition sequences, and a thin section of 5 mm to ensure that macroscopic intravoxel dephasing did not occur in the section selection direction.

Signal intensity in regions of interest that encompassed the central 80% of the cross-sectional area of each tube were measured. In all cases, corrections for radio frequency coil homogeneity were made based on measurements at the same geometric locations in a large homogeneous phantom. Corrections for background signal intensity were calculated using a method previously described (7). Measurements of background intensity were made in the corner of the image away from any artifacts.

Relaxation times were measured as follows: T1 was measured with repeated saturation-recovery spin-echo sequences with a TE of 12 msec and a TR of 50, 100, 200, 400, 800, 1600, and 3200 msec. The T1 values were extracted using a three-parameter least-squares fit to measurements of image intensity. T2 was measured using a single section optimized Carr-Purcell-Meiboom-Gill MR sequence with a TR of 1000 msec and 16 echoes evenly spaced between 0 and 240 msec (8). Single-component T2 values were extracted using two-parameter least-squares fit to the data. M_o values (the relative proton density) were extrapolated from the T1 data using appropriate corrections for the T2 decay during the TE at 12 msec and were also extrapolated from the T2 data using appropriate corrections for the lack of T1 recovery during a TR of 1000 msec. The M_o values at each concentration of calcium were averaged to determine the proton density dependence on calcium concentration.

T2* values were obtained from a gradient-recalled acquisition in the steady state (GRASS) (9) sequence with a TR of 1500 msec, flip angle of 30°, and TE of 5, 7.5, 10, 12.5, 15, 17.5, 20, 22.5, 25, 30, and 40 msec. The regions of interest from each tube were fit to a single component T2* decay with the same fitting routine as the T2. These data were also analyzed in terms of the signal difference between each calcium concentration and that of agarose gel without calcium to determine which TE gave maximum contrast. This value of TE (20 msec in the phantom experiments) was used for the remainder of the measurements.

With the preliminary characterization of the phantom complete, spoiled GRASS (SPGR) images (or equivalently fast low-angle shot (FLASH) [10]) were taken of the phantom with TR values of 30, 100, and 500 msec representing short, intermediate, and long TR values using 8, 4, and 1 excitations, respectively, to ensure that good signal-to-noise ratio was obtained in every experiment. For each TR, images were acquired with flip angles of 5°, 10°, 15°, 20°, 25°, 30°, 40°, 50°, and 60°. Transmitter and receiver gains were kept constant to ensure that quantitative measurements could be compared. After completion of the 3 × 9 = 27 SPGR images, the complete experiment was repeated with single-section GRASS and the same timing parameters.

Theoretical signal intensity was calculated for each of the SPGR measurements using previously reported equations for signal intensity for spoiled FLASH or spoiled GRASS sequences (11, 12). The expression used was:

$$S(TR, TE, \alpha, Ca) = kM_o[Ca]e^{-R*_2[Ca]TE}B \int_{-z_{max}}^{z_{max}} \sin(\alpha(z)) \frac{1 - e^{-R_1[Ca]TR}}{1 - \cos(\alpha(z))e^{-R_1[Ca]TR}} dz. \quad (1)$$

The parameter k is an arbitrary constant relating measured ROI to spins in a voxel of water. $M_o[Ca]$, $R*_2[Ca]$, and $R1[Ca]$ are the values of the proton density, 1/T2* and 1/T1 measured at each calcium concentration. α is the effective flip angle for each position z through the section thickness. B accounts for the section profile shape and is chosen so that the maximum section intensity is 1 for α tuned to give maximum signal in the transverse plane with TR infinitely large. The range $-z_{max} < z < z_{max}$ covers the section profile.

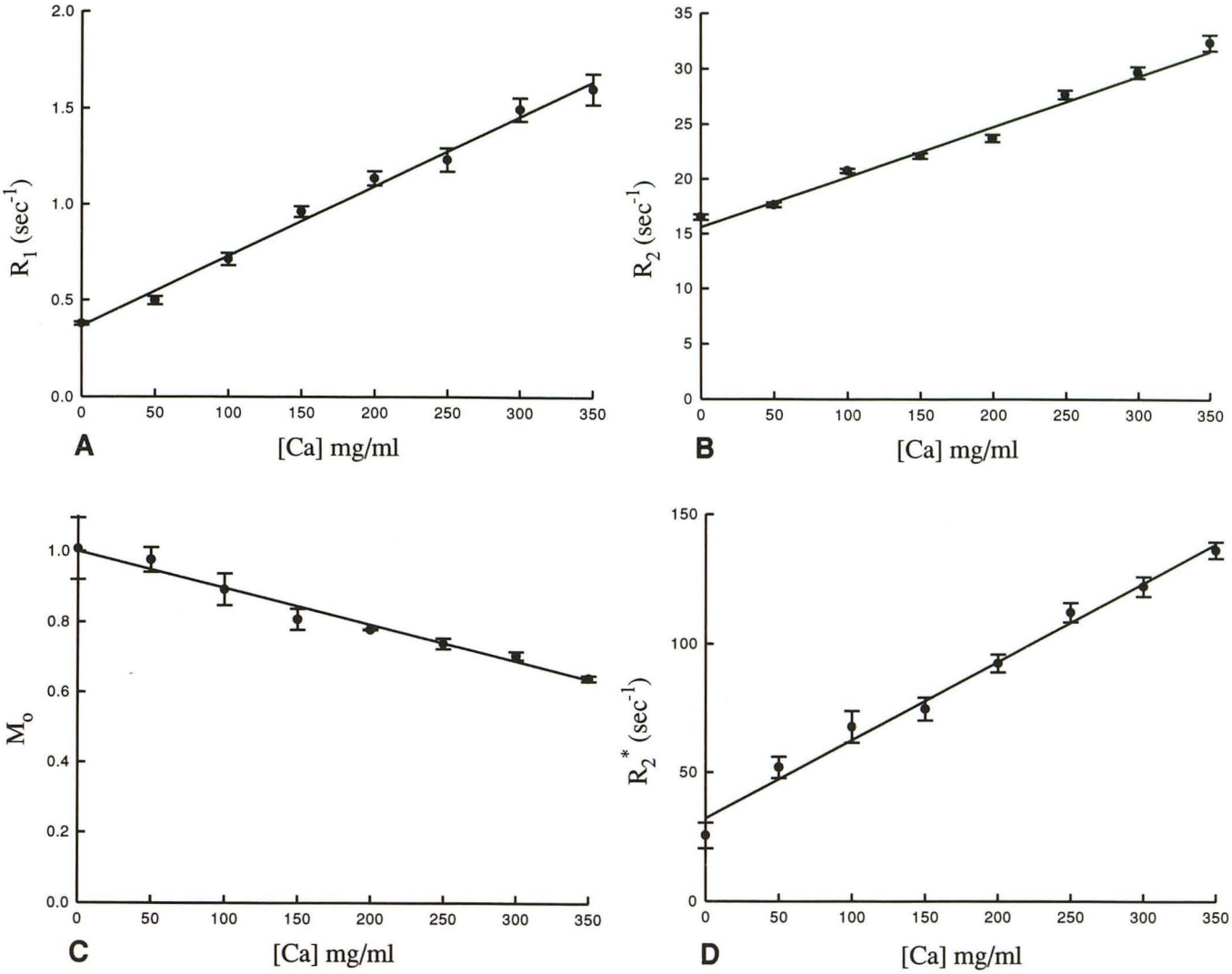

Fig. 1. Measured relaxation rates as a function of calcium concentration for *A*, T1; *B*, T2; *D*, T2*. *C* shows the relative spin density, which decreases as the calcium concentration increases. The data points are experimental and the error bars representing the standard deviations of the fitted experimental rates. The straight lines on the graphs are linear regressions for which the parameters are summarized in Table 1.

For the calculations presented in this paper, the radio frequency excitation pulse is taken to be a single-lobed sinc pulse multiplied by a Hamming filter ranging from 1.0 at the center of the radio frequency pulse down to 0.08 at the second zero crossing of the sinc function. Because the flip angles of importance in this experiment are small, the nonlinearities of the Bloch equations are ignored and the flip angle profile $\alpha(z)$ is taken to be the Fourier transform of the radio frequency excitation pulse.

The T1 and T2* values for normal brain were measured in a volunteer and the results were used with the established signal intensity equations to determine optimal gradient-echo sequences for visualizing calcium in the brain. The optimal sequence was used to examine a patient, with multiple intracerebral calcifications caused by cysticercosis. TR, TE, and flip angle were varied for comparison purposes.

Results

The physical characterization of the phantom parameters are shown in Fig 1. In all cases, the decay (or recovery) curves deviated from a monoexponential, as has been reported previously (6). However, for simplicity, only average relaxation rates are presented in this figure. The relaxation rates and the proton density are shown to be

TABLE 1: Linear regression relationships characterizing calcium doped gels as a function of solute concentration

$R1 = \frac{1}{T1} = 0.003.6\ [Ca] + 0.365\ sec^{-1}$
$R2 = \frac{1}{T2} = 0.046\ [Ca] + 15.6\ sec^{-1}$
$R2^* = \frac{1}{T2^*} = 0.305\ [Ca] + 32.0\ sec^{-1}$
$Mo[Ca] = Mo(0.001-1.0\ [Ca])$

Note.—The concentration of calcium [Ca] is expressed in milligram per milliliter of gel solution.

linear functions of the concentration of calcium. On the GRASS images, the signal difference between various concentrations of calcium and the zero concentration gel phantom were evaluated as a function of TE. Although the TE time for maximum contrast decreases slightly with increasing calcium concentration, the contrast at a TE of 20 msec for all concentrations exceed 90% of its maximum value. Thus, the remainder of the experiments were performed with a fixed TE of 20 msec. It should be noted, however, that the optimal TE will be longer with lower calcium concentrations and will also depend on the T2* of the background tissue.

Figure 2 shows the SPGR signal intensity measured in each tube with varying calcium concentration for a short, intermediate, and long TR value as a function of flip angle. The data points are measured from the images and the lines are calculated using the equation presented in the methods section. The actual R1 and R2* values that were measured for this same section and which are shown in Fig 2 were used for the calculated lines. The only free parameter is k, the scaling between the theoretical magnetization (normalized to 1 for water with a TE of 0 and a TR at ∞) and the measured regions of interest. It was determined to have a value of 3795 by least-squares fit to the 216 data points.

In general, there is very good agreement between the experiment and theoretical expressions. The greatest discrepancies occur with large flip angles, for which the assumption of the linearity of the Bloch equations is least valid. However, because the calculations are subsequently used for small flip angles, the agreement is more than adequate. For short TR times (30 msec), the maximum signal occurs with small flip angles (5 to 10°). However, for long TR times (500 msec), the total signal intensity is much larger and the optimum flip angle increases to the 25° to 40° range.

The results with the GRASS sequence that is not spoiled are shown in Fig 3. For TR of 100 msec and 500 msec, the GRASS signal intensities did not differ significantly from the SPGR results. This is expected because the susceptibility effects shorten T2* to a level at which the transverse magnetization at TR greater than 100 msec has been effectively reduced below 2% for calcium concentrations even as low as 50 mg/mL. Thus, for steady-state sequences such as GRASS, the inhomogeneity serves to dephase the transverse magnetization, making the signal intensities equivalent to SPGR except in the case of very short TR (30 msec), as shown in Fig 3. The signal is greater for the low concentration of calcium at larger flip angles in the GRASS sequences than in the SPGR sequence because residual magnetization is maintained and not dephased; with a TR of 30, some of the transverse magnetization remaining before any radio frequency excitation is added to the new transverse magnetization generated by the next flip angle pulse. However, in the region where calcium contrast is maximum (flip angle between 5° and 15°), the GRASS and SPGR sequences behave essentially equivalently.

Having demonstrated the validity of Equation 1 to describe accurately the experimental results in a phantom, we use the mathematical expression for signal intensity to optimize the pulse sequence to obtain maximum calcium contrast in brain imaging. For applications to human brain imaging, the T1 and T2* of healthy volunteer brain (average of gray and white matter) were measured to be 910 ± 20 msec and 59 ± 5 msec, respectively. Assuming that the relaxivity of calcium in the brain is the same as that demonstrated in the calcified gel samples, then the relaxation rates of calcified brain ([Ca] is the calcium concentration in milligrams per milliliter) would be expected to be

$$R_1 = 0.0036\ [Ca] + 1.10\ sec^{-1} \quad \text{and} \quad R_2^* = 0.305\ [Ca] + 17\ sec^{-1}.$$

For each choice of TR and [Ca], the flip angle and TE values that maximize the contrast efficiency are determined. The contrast efficiency is defined as the signal difference per square root of time and is given by:

$$\text{efficiency} = \frac{S(Ca = 0) - S(Ca)}{\text{time}}.$$

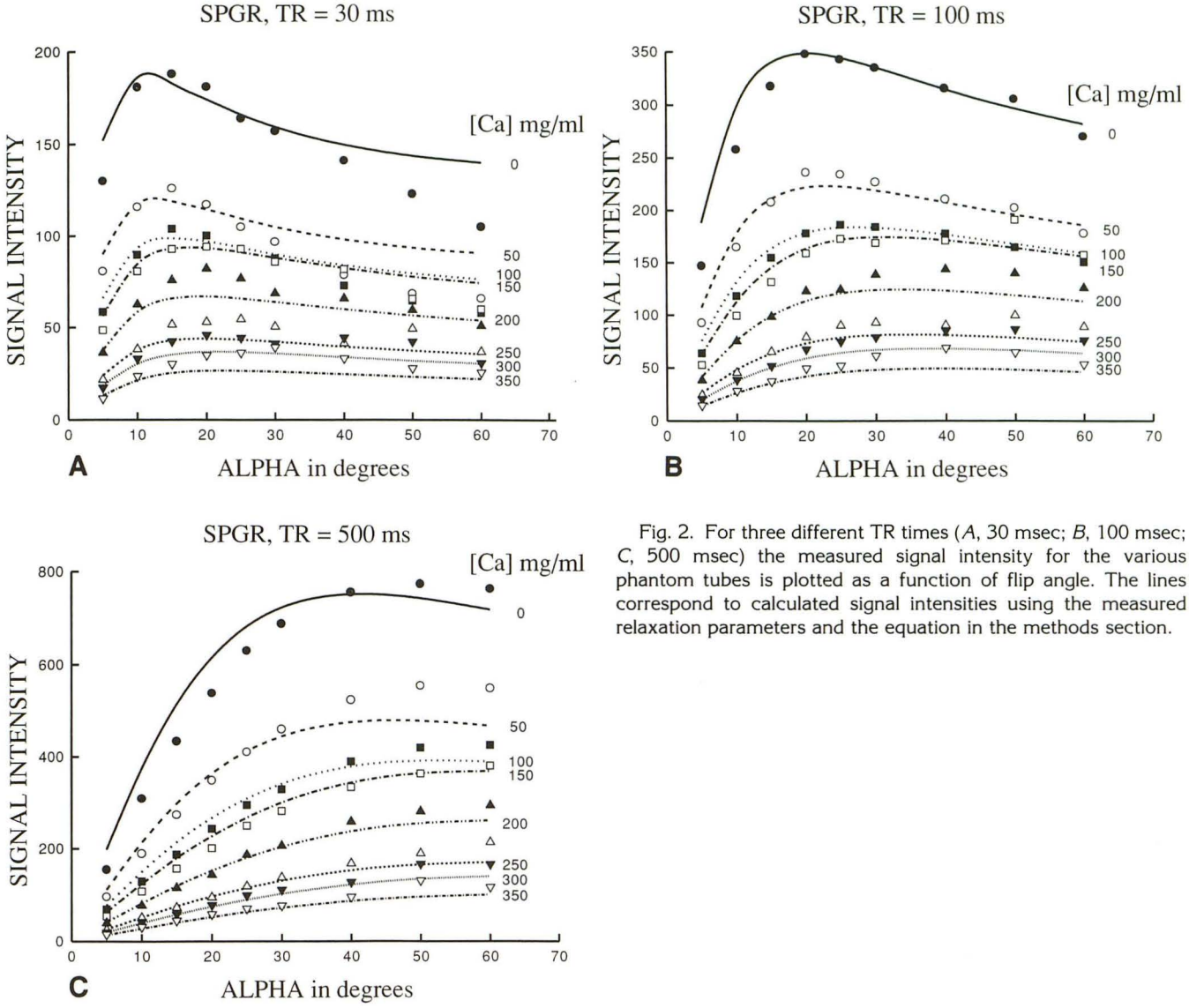

Fig. 2. For three different TR times (*A*, 30 msec; *B*, 100 msec; *C*, 500 msec) the measured signal intensity for the various phantom tubes is plotted as a function of flip angle. The lines correspond to calculated signal intensities using the measured relaxation parameters and the equation in the methods section.

The square root of time (the total time to acquire the image) is included to ensure that the signal difference-to-noise ratio achievable per equivalent duration of imaging time are being compared (13). As has been noted previously (14), the achievable contrast efficiency is relatively independent of TR provided TR is less than T1 and provided optimal flip angles are used. Provided TE is between 26 and 32 msec, for all calcium concentrations from 50 to 300 mg/mL, 90% of the maximum possible contrast will be obtained for flip angle values within the range shown in Fig 4. Fortunately, the flip angles and TEs that maximize the signal-to-noise ratios for differing concentrations of hydroxyapatite are relatively, but not totally, independent of calcium concentration as shown in Table 2. This allows sequences to be defined that are near maximally effective in searching for calcification even when the degree of calcification is not known. Because the contrast efficiency is independent of TR (provided the appropriate flip angle is used), the repetition time can be selected on the basis of patient throughput, motion artifacts, numbers of sections required, and image contrast desired for the brain.

The images of the patient examined with a variety of TRs, TEs and flip angles demonstrated (Fig 5) that abnormal calcified tissue is evident on all the gradient-echo images, more so on some than on others. There was little dependence on flip angles with respect to lesion contrast. The best contrast was on the image for which flip angle was optimized for TR to give the greatest normal brain signal, but the difference was small (Fig 5*B* compared with 5*A* and 5*C*). Of all the

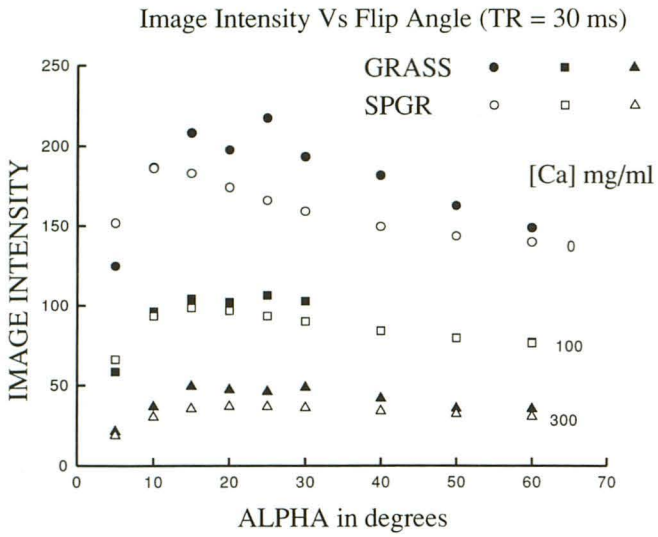

Fig. 3. For a TR of 30 msec, the SPGR results (open symbols) are compared with the unspoiled GRASS results (solid symbols). At large flip angles and small calcium concentrations, the unspoiled sequence gives slightly higher signal intensity. However, the differences are not sufficiently large to be important.

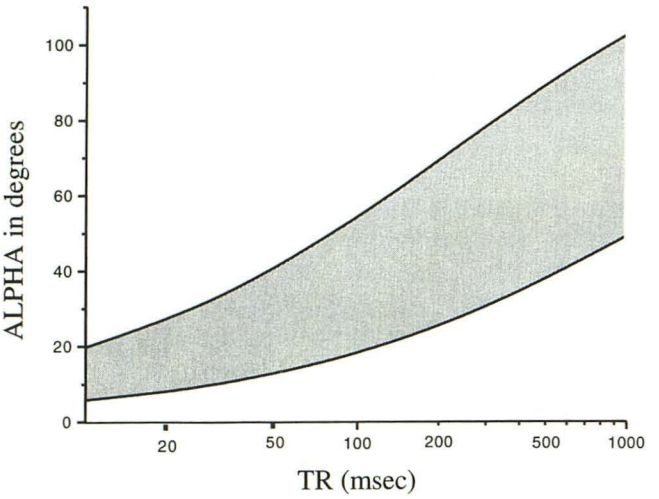

Fig. 4. For all calcium concentrations from 0.10 to 0.30 g/mL, the contrast efficiency is within 90% of its maximum value provided the flip angle (in degrees) for each TR value (in milliseconds) is selected between the two solid lines.

TABLE 2: Maximum lesion contrast in brain as a function of calcium concentration ([Ca]) and echo time (TE)

[Ca] (mg/mL)	Optimum TE (msec)	Range of TE (msec)
50	43	26–65
100	34	21–53
200	24	14–39
300	19	11–32

Note.—Maximum image contrast in brain is achieved at the "optimum TE." Any TE within the "range of TE" will achieve ≥90% of the maximum image contrast. Note that TE at 26 to 32 msec is within the 90% range for all calcium concentrations, and also note that lesser calcium concentrations, require longer TEs to achieve the very best image contrast.

gradient-echo methods tested, those with flip angles smaller than the calculated optimum and at TEs shorter than the optimum made the smaller lesions least evident. Examination of the images at longer than optimal TEs with which the smallest lesions were most apparent is particularly interesting (Figs 5*E* and 5*F*). We presume that the slight improvement in image contrast for the smallest lesions at larger TEs indicates that these have the lowest calcium concentration (Table 2). At a TE of 66 msec, susceptibility artifact at the brain-skull interface is so great that the peripheral part of the brain is degraded below diagnostically acceptable levels, and the lesions show susceptibility artifacts (14).

Discussion

Particulate material that is either diamagnetic or paramagnetic leads to susceptibility dephasing and shortening of T2*. Gradient-echo imaging does not use a refocusing radio frequency pulse and is therefore the best method of detecting this T2* effect. The voxel containing the particulate material and, potentially, the neighboring voxels display loss of signal intensity. In clinical MR, knowledge of this effect may be used to advantage to visualize subtle calcification that may otherwise escape detection (1). Intuitively it stands to reason that the greater the degree of hypointensity of the area in question relative to the normal surrounding tissue (the image contrast), the more easily the lesion will be detected.

Gradient-echo imaging has three important operator-selected variables that control image contrast: TE, flip angle, and TR. For calcium, the manner in which signal intensity and image contrast vary with these parameters is not intuitively obvious.We investigated systematically the dependence of signal intensity and image contrast on each of these variables, both experimentally and theoretically. The excellent agreement between calculation and measurements in the phantom allowed us to predict theoretically a spectrum of optimal gradient-echo imaging sequences for detecting calcium in the brain.

The resulting recommended pulse sequences can be understood qualitatively. Susceptibility dephasing leads to T2* shortening and a loss of signal in and around calcified lesions. Increasing TE beyond an optimum leaves the lesion black but decreases the signal from brain, diminishing the contrast. Furthermore, excessively long TEs lead to substantial susceptibility-induced signal loss at interfaces and other artifacts that make

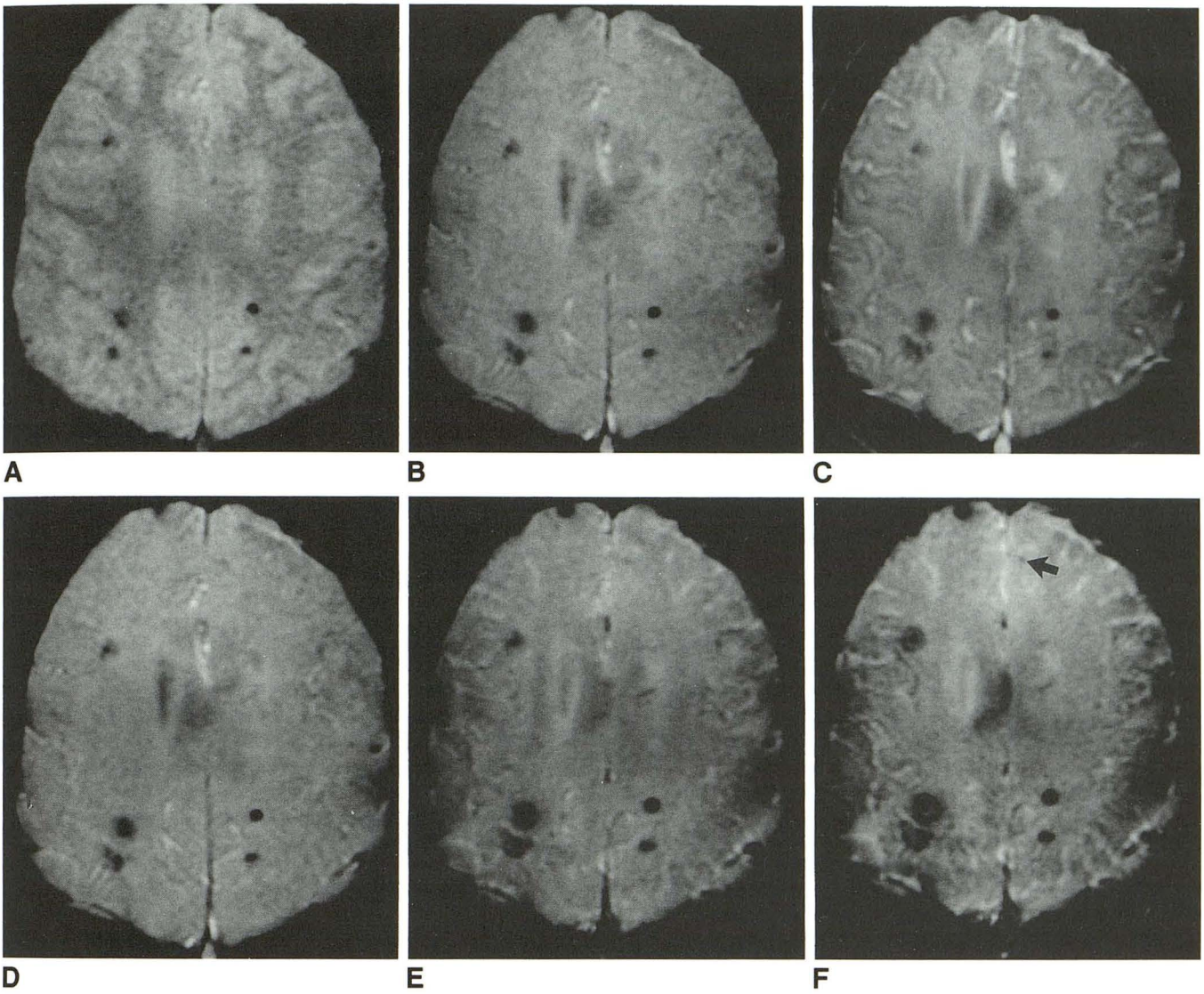

Fig. 5. Cysticercosis with multiple intracerebral calcifications. TR, TE, and flip angle vary between each image. Multiple hypointense lesions are evident on all images representing dystrophic calcification secondary to the cysticercal infection.

A–C, TR and TE are kept constant (TR at 120 msec, TE at 22 msec) and flip angle is varied from 10° (*A*), to 33° (*B*), to 70° (*C*). Five hypointense lesions are clearly visible on each image. The average contrast (background tissue signal minus lesion signal) is best appreciated in *B* both qualitatively and quantitatively. The basic type of image contrast of the brain does change markedly; *A* is proton density–weighted, *B* has flat contrast, *C* is mostly T1-weighted except for cerebrospinal fluid, which has high signal because of steady-state effects. *D–F,* TR and flip angle are kept constant (TR at 120 msec, flip angle at 33°) and TE is varied from 22 (*D*) to 44 (*E*) to 66 msec (*F*). Five lesions are very evident on every image, a sixth becomes convincing with the longest TE (*arrow*) (*F*). For each lesion contrast is quantitatively better on *E* and *F* than on *D*. Also, the apparent size of the lesion appears to grow as TE gets longer. By TE at 66 msec, (*F*) some artifactual substructure is appearing within the lesions (14) and susceptibility-induced signal loss at the brain-skull interface degrades the quality of this image to the point where it is diagnostically unacceptable. *D* would be the best compromise between lesion visibility and acceptable signal loss of the skull interface. We speculate that the greater image contrast seen with the TE of 44 msec (*E*) is caused by the calcium present within the lesions was less than 100 mg/mL. Although this cannot be proved in a clinical case, it is consistent with the calculations shown in Table 2.

the images diagnostically useless. Thus, we recommend 29 msec as an optimum TE for gradient imaging with a slightly longer value for concentrations less than 100 mg/mL.

The recommended flip angle is related to the TR value. For spoiled GRASS or FLASH imaging at a given TR, there is an optimum flip angle that maximizes the MR signal (15, 16) given by the Ernst angle: flip $\text{angle}_{\text{optimum}}$ = arc cos [exp(−TR/T1)]. The recommended flip angle as a function of TR shown in Fig 4 is basically a reflection of the Ernst angle, but differs somewhat in that it includes the effects of section profile and calcium contrast. Spoiled gradients in the

gradient-echo sequence have been shown to have insignificant effect because the susceptibility dephasing effectively spoils the transverse magnetization. Thus, the decision of whether to use GRASS or SPGR and the specific selection of TR can be determined by the desired appearance and coverage of the normal brain.

In summary, a gradient-echo sequence can be designed to optimize the image contrast of calcified tissue. The sequence can be spoiled or unspoiled, and should have a TE of 29 msec or longer and a flip angle related to the choice of TR as dictated in Fig 4.

Acknowledgments

Financial support from the National Cancer Institute of Canada, General Electric Medical Systems of Canada, and Berlex Canada is gratefully acknowledged. John Watts assisted with the phantom preparation and imaging experiments; Dr Peter Stanchev completed the numerical calculations and data fitting.

This work was supported by the National Cancer Institute of Canada and General Electric Medical Systems of Canada. Walter Kucharczyk is supported by a Career Investigator Award from Berlex Canada Inc.

References

1. Atlas SW, Grossman RI, Hackney DB, et al. Calcified intracranial lesions: Detection with gradient-echo-acquisition rapid MR imaging. *AJNR Am J Neuroradiol* 1988;9:253–261
2. Nixon JR, Houser OW, Gomez MR, Okazaki H. Cerebral tuberous sclerosis: MR imaging. *Radiology* 1989;170:869–875
3. Lang C, Huk W, Pichl J. Comparison of extensive brain calcification in postoperative hypoparathyroidism on CT and NMR scan. *Neuroradiol* 1989;31:29–36
4. Dell LA, Brown MS, Orrison WW, et al. Physiologic intracranial calcification with hyperintensity on MR imaging: case report and experimental model. *AJNR Am J Neuroradiol* 1988;9:1145–1150
5. Holland BA, Kucharczyk W, Brant-Zawadzki M, Norman D, Haas DK, Harper PS. MR imaging of calcified intracranial lesions. *Radiology* 1985;157:353–357
6. Henkelman RM, Watts J, Kucharczyk W. High signal intensity in MR images of calcified brain tissue. *Radiology* 1991;179:199–206
7. Henkelman RM. Measurements of signal intensities in the presence of noise in MR images. *Med Phys* 1985;12:232–233
8. Poon CS, Henkelman RM. Practical T_2 imaging for clinical applications. *J Magn Reson Imaging* 1992;2:541–553
9. Haase A, Frahm J, Matthaei D, Hänicke W, Merboldt KD. FLASH imaging: rapid NMR imaging using low flip angle pulses. *J Magn Reson* 1986;67:258–266
10. Crawley AP, Wood ML, Henkelman RM. Elimination of transverse coherences in FLASH MRI. *Magn Reson Med* 1988;8:248–260
11. van der Meulen P, Groen JP, Tinus AMC, Bruntink G. Fast field echo imaging: an overview and contrast calculations. *Magn Reson Imaging* 1988;6:355–367
12. Zur Y, Stokar S, Bendel P. An analysis of fast imaging sequences with steady-state transverse magnetization refocusing. *Magn Reson Med* 1988;6:175–193
13. Henkelman RM, Hardy P, Poon PY, Bronskill MJ. An optimal MRI sequence for imaging hepatic metastases. *Radiology* 1986;161:727–734
14. Kim JK, Kucharczyk W, Henkelman RM. Dipolar susceptibility artifacts from cavernous hemangiomas. *Radiology* 1993;187:735–741
15. Bendel P. T_2-weighted contrast in rapid low flip-angle imaging. *Magn Reson Med* 1987;5:366–370
16. Ernst RR, Anderson WA. Fourier transform NMR spectroscopy. *Rev Sci Instrum* 1966;37:93–102